

Insight on the exceptional indentation strength of graphite under cold compression

Xiang-Feng Zhou¹, Xiao Dong¹, Guang-Rui Qian³, Yonjun Tian², and Hui-Tian Wang^{1,3}

¹School of Physics and Key Laboratory of Weak-Light Nonlinear Photonics, Ministry of Education, Nankai University, Tianjin 300071, China

²State Key Laboratory of Metastable Materials Science and Technology, Yanshan University, Qinhuangdao 066004, China

³Nanjing National Laboratory of Microstructures, Nanjing University, Nanjing 210093, China

Abstract

By performing first-principle calculations, we showed a new body centered tetragonal carbon polymorph (named as Bct-Carbon), as believed experimentally but never confirmed. Both the phase transition pressure and the simulated X-ray diffraction pattern for the Bct-Carbon are in good agreement with experimental results [W. L. Mao *et al.*, *Science* **302**, 425 (2003)]. Most importantly, the lowest activation barrier of Bct-Carbon compared with that of M-Carbon [Q. Li *et al.*, *Phys. Rev. Lett.* **102**, 175506 (2009)] or diamond implies that it will be easier to form from graphite and the highest shear strength (109 GPa) of Bct-Carbon could be used to reveal the exceptional indentation strength that can crack diamond.

Carbon exists in a large number of forms owing to the flexibility of carbon to form sp -, sp^2 -, and sp^3 -hybridized bonds, such as graphite, hexagonal diamond (lonsdaleite), diamond, nanotubes, fullerenes, and amorphous carbon [1-5]. The cubic diamond phase of carbon remains the hardest elemental solid at room temperature. Because of its extensive application, much intense theoretical and experimental efforts have been devoted to searching materials that are harder and thermally more stable than diamond [6, 7]. Indeed, some polycrystalline samples that transferred from graphite under high pressure and high temperature (HPHT) are reported to have the same or higher hardness compared with single crystal diamond [7]. Recent the cold-compressed experiments indicate new carbon polymorphs exhibit exceptional indentation strength which is capable of indenting diamond anvils [4, 5]. Some samples could be quenchable at room temperature [5]; the others are not [4]. Especially for the graphite, it is originally an ultrasoft material under ambient condition due to the weak van der Waals interactions among the interlayers, but shows giant shear strength enhancement under the cold compression [4]. Such an unexpected enhancement raises many fundamental questions: What is the exact crystal structure during the phase transition, and what novel character result in the exceptional indentation strength. It was initially considered as hexagonal diamond, an intermediate or modified hexagonal phase between graphite and diamond, or an amorphous phase [1, 2, 8]. Instead of those findings, Li *et al.* found the mixture of graphite and M-carbon could explain better the X-Ray diffraction (XRD) pattern and the near K-edge spectroscopy by using the *ab initio* evolutionary algorithm [9]. However, the relative lower calculated bulk modulus (431 GPa) and hardness (83 GPa) did not provide strong evidence to unveil the exceptional indentation strength that can crack diamond [4]. Therefore, more extensive explorations needed to resolve these ambiguities.

In this letter, we employ the *ab initio* pseudopotential density functional method in CASTEP code within the local-density approximation (LDA) to carry out first-principles calculations [10]. The norm-conserving pseudopotentials are used and expanded by a plane-wave basis set with a cutoff energy of 660 eV and the Monkhorst-Pack Brillouin zone sampling grid spacing of 0.04 \AA^{-1} . The

electron-electron exchange interaction is described by the exchange-correlation function of Ceperley and Alder as parameterized by Perdew and Zunger [11]. During the geometry optimization, no symmetry and no restriction were constrained for both the unit cell shape and the atomic positions with respect to the Brodyden-Fletcher-Goldfarb-Shanno (BFGS) minimization scheme. The structural relaxation was stopped until the total energy, the maximum ionic displacement, and the maximum stress the maximum ionic Hellmann-Feynman force were within 5×10^{-6} eV/atom, 0.01 eV/Å, 5×10^{-4} Å, and 0.02 GPa, respectively. The tensile and shear stress are computed as follows: We first set the desired component of the target stress at a certain value and all the other components at zero, then relax both the lattice vectors and atomic positions simultaneously. After getting the final structure with the given stress, we increased the desired stress step by step until the structure collapse, and then the maximum stress was considered as the ideal strength [12-15]. The simulated XRD was calculated by the Reflex module.

We performed routine first-principle calculations to help clarify the high-pressure phases of carbon. Our searches involve relaxing set of randomly chosen structures or modifying ones that constructed from different orientation of prototype crystal to minima in the energy at ground state or fixed pressure [16, 17]. A novel carbon phase with tetragonal symmetry (I4/mmm, space group number 139) is achieved by using the above mentioned method. The lattice parameters are $a = b = 4.322$ Å and $c = 2.478$ Å, a nonidentical C atom occupy the 8h (0.18, 0.18, 0) site. Due to the similar structural motif [see Fig. 1 (a), (b) and (c)] compared with the published body-centered tetragonal polymorph of zinc oxide (Bct-ZnO) [18]. Therefore, we named our structure as Bct-Carbon. Remarkably, the calculated phase transition pressure from graphite to Bct-Carbon is 20.8 GPa compared with 15.2 GPa for the M-Carbon (see from the inset of Fig. 2). In order to check the reliability of our results, we also adopted the same VASP code and parameters to get the transition pressure for the M-carbon and Bct-Carbon [19], the corresponding values are 18.6 and 13.7 GPa, respectively. Therefore, both of them have been shown the transition pressure of Bct-Carbon is in excellent agreement with experimental result (about 17 GPa) [4].

Most importantly, the calculated activation barrier of diamond is 0.071 eV/atom compared with graphite (see Fig. 2), which qualitatively agree with the previously calculations [20]. The corresponding value of M-carbon is only 0.033 eV/atom, which is in satisfactory agreement with Liang's result (0.018 eV/atom) that M-Carbon has the lowest activation barrier among cubic diamond, hexagonal diamond, and K₄ carbon [21]. Strikingly, the energy barrier of Bct-Carbon (0.017 eV/atom) is only half of M-Carbon (0.033 eV/atom). It indicates Bct-Carbon will be easier to form from graphite, meanwhile, cannot be quenchable at room temperature. It is consistent with experimental observation [4]. In fact, this extreme energy barrier could be easily understood from the crystallography of Bct-Carbon: The atomic arrangement in Bct-Carbon formed the fluctuant graphene-like motif if we viewed from the projection of (001) or (010) plan [Fig. 1 (a) and (b), both of them should be identical]. These graphene-like structures will be bonded directly from [100] or [010] (identical) direction during the cold compression, and finally formed the "4+8" structure [see Fig. 1 (c)] compared with "5+7" structure of M-Carbon [22]. Therefore, Origin of the lowest energy barrier of Bct-Carbon is getting over the weak van der Waals interactions along [100] or [010] direction. The novel "4+8" motif of Bct-Carbon also provides direct theoretical evidence for Mao's prediction [see Fig. 2 of the reference (4)] that the bridging carbon atoms paired with other atoms in the adjacent layers to form σ bonds upon compression. The remaining π^* component in the near K-edge spectrum is coming from the incomplete conversion from graphite [9].

To further confirm our structural model, we have simulated the XRD patterns to compare with that of M-Carbon and experiment. Fig. 3 (c) shows the simulated XRD patterns of graphite under 3.3 and 13.7 GPa, both the peak positions and intensities are in good agreement with the experimental data [4]. It also should note that the difference between theory and experiment in the range of 10° -15° indicates that the background noise in experiment will lead to undetectable measurement for some very weak positions. The key problem is located at the transition point (18.4 GPa), two distinct strong peaks [100 and 110 peak, depicted by black line from Fig. 3(b)] at 9°

and 15.5° match the experimental data extremely well [4]. The 002, 101 and 112 peaks are most likely attributed from graphite or M-Carbon. Considering there is a shift for the transition pressure between theory and experiment, it is very difficult to distinguish the exact peaks to some extent because almost all of peaks for Bct-Carbon could be hidden among the reflections of the M-Carbon. There is the same trend at 23.9 GPa, the intensity of graphite should have decreased with the increasing pressure due to more graphite has been converted to Bct-Carbon or M-Carbon. As a matter of convenience, we just keep the constant weight (50% of graphite) for the simulation [9]. Owing to the great overlap for the peaks among these phases, such as 002, 100, and 101 positions, the mixture of three phases could explain the broad experimental peaks. The ambiguities in the experiment have been interpreted self consistently, and Bct-Carbon has been confirmed to be the intermediate phase upon cold compression.

We now focus on the super indentation strength of graphite under cold compression. By using methods that involve applying a given homogeneous deformation (strain) and calculating the resulting stress for the fixed unit cell, nine nonzero elastic constants will be determined. Combined with Voigt-Reuss-Hill approximation [23], we applied it to the diamond, and the calculated bulk modulus and shear modulus are 447 and 540 GPa, respectively. These values are in good agreement with experimental results (442, 544 GPa) [24]. Using the same method, the corresponding values of Bct-Carbon are 414 and 427 GPa which is lower than that of diamond; thereby it seems that Bct-Carbon will be not harder than diamond, just as M-Carbon (415, 468 GPa). However, it is well known that bulk and shear modulus do not necessarily give an accurate account for materials strength. This is because these elastic constants are evaluated at the equilibrium state, and materials deformations associated with the cold compression measurements usually involve large strains where bonding characteristics may change greatly [14]. Thus the ideal strength calculation should be a good alternative method to estimate the indentation strength. We first test the diamond (see Fig. 4), the tensile and shear strength along the weakest direction are 91.1 GPa and 92.5 GPa at strain ε of 0.13, 0.27 accordingly, which is consistent with

previous calculations [12-15]. These results are compared the one we obtain for the Bct-Carbon. In the case of a tensile load along the [100], [010], [001], [110], and [111] directions, we find the tensile stress are 84.8, 84.8, 139.7, 131.1, and 107.5 GPa, respectively. Therefore, the weakest direction is [100] or [010]; both two directions are identical [see Fig. 1 (c)]. The ideal tensile strength (84.8 GPa) is lower than that of diamond (91.1 GPa), which implies Bct-Carbon will be easier to cleave than diamond. To explain the ring crack indentation on the diamond anvils, shear strength, which relates to the resistance to indentation, is more fundamental. Given that [010] direction is the weakest tensile direction, we further explore the case of shearing, and verify the shear strength of (001) [100], (001) [010], (010) [100], (010) $[00\bar{1}]$, and (010) [001] are 108.6, 108.6, 119.7, 108.6, and 108.6 GPa, respectively. Therefore, (010) [001] (or other identical shear directions) system will be the weakest slip system, and the ideal shear strength (108.6 GPa) in Bct-Carbon is large by at least 17% than that of diamond (92.5 GPa). Inset of Fig. 4 shows the snapshot of Bct-Carbon at the shear stress of 108.6 GPa, the weakest C-C bond (1.669 Å) would not break up upon the large strain ($\varepsilon=0.29$), which denote the great endurance beyond the linear elastic regime. It will finally collapse to the graphite when increasing strain or stress subsequently. Note that there are two different kinds of C-C bonds in Bct-Carbon with the bond length of 1.559 and 1.503 Å at equilibrium state, the average bond length is 1.531 Å compared with that of diamond (1.527 Å), which imply Bct-Carbon has the similar bond strength as diamond [25]; thus the exceptional shear strength could not be analyzed by its equilibrium or elastic properties completely. In fact, the proposed “crystallographic strength” could be expected to interpret the giant indentation strength which can crack diamond because the Bct-Carbon has the perpendicular graphene-like structure [see Fig. 1 (a), (b), and (c)], and graphene has been proved to be the hardest materials with the strongest intrinsic bond strength [26]. The novel crystal structure of Bct-Carbon determines this exceptional shear strength due to the perpendicular graphene-like configuration could withstand the larger critical stress from different directions. Therefore, mechanisms for the anomalous enhancement of

indentation strength have been clarified, which also provide good example to design superhard materials not only from the bond length (bond strength) but also from the bond network (crystallographic strength) [27].

In conclusion, we have shown a new carbon phase which is interpreted as superhard graphite upon cold compression. Because it has good transition pressure, simulated XRD pattern, and the lowest activation barrier, it unveils the novel formation process of superhard graphite. In particular, the perpendicular graphene-like structure of Bct-Carbon results in the exceptional shear strength that can crack diamond.

This work was supported by the National Natural Science Foundation of China under Grant NO. 50532020, by the 973 Program of China under Grant No. 2006CB921805 and 2005CB724400, the Postdoctoral Fund of China under Grant No. 20090460685.

References

- [1] E. D. Miller, D. C. Nesting, and J. V. Badding, *Chem. Mater.* **9**, 18 (1997).
- [2] T. Yagi, W. Utsumi, M. Yamakata, T. Kikegawa, and O. Shimomura, *Phys. Rev. B* **46**, 6031 (1992).
- [3] J. R. Patterson, A. Kudryavtsev, and Y. K. Vohra, *Appl. Phys. Lett.* **81**, 2073 (2002).
- [4] W. L. Mao, H. K. Mao, P. J. Eng, T. P. Trainor, M. Newville, C. Kao, D. L. Heinz, J. Shu, Y. Meng, and R. J. Hemley, *Science* **302**, 425 (2003).
- [5] Z. Wang, Y. Zhao, K. Tait, X. Liao, D. Schiferl, C. Zha, R. T. Downs, J. Qian, Y. Zhu, and T. Shen, *Proc. Natl. Acad. Sci. U.S.A.* **101**, 13699 (2004).
- [6] D. M. Teter and R. J. Hemley, *Science* **271**, 53 (1996).
- [7] T. Irifune, A. Kurio, S. Sakamoto, T. Inoue, and H. Sumiya, *Nature* **421**, 599 (2003).
- [8] F. J. Ribeiro, P. Tangney, S. G. Louie, and M. L. Cohen, *Phys. Rev. B* **72**, 214109 (2005).
- [9] Q. Li, Y. Ma, A. R. Oganov, H. Wang, H. Wang, Y. Xu, T. Cui, H. K. Mao, and G. Zou, *Phys. Rev. Lett.* **102**, 175506 (2009).
- [10] M. Segall, P. Lindan, M. Probert, C. Pickard, P. Hasnip, S. Clark, and M. Payne, *J. Phys.: Cond. Matt.* **14**, 2717 (2002); <http://accelrys.com>
- [11] D. M. Ceperley, and B. J. Alder, *Phys. Rev. Lett.* **45**, 566 (1980); J. P. Perdew, and A. Zunger, *Phys. Rev. B* **23**, 5048 (1981).
- [12] R. H. Telling, C. J. Pickard, M. C. Payne, and J. E. Field, *Phys. Rev. Lett.* **84**, 5160 (2000).
- [13] H. Chacham, and L. Kleinman, *Phys. Rev. Lett.* **85**, 4904 (2000).
- [14] Y. Zhang, H. Sun and C. F. Chen, *Phys. Rev. Lett.* **93**, 195504 (2004).
- [15] S. Y. Chen, X. G. Gong, and S. H. Wei, *Phys. Rev. Lett.* **98**, 015502 (2007).
- [16] X. F. Zhou, J. Sun, Y. X. Fan, J. Chen, H. T. Wang, X. J. Guo, J. L. He, and Y. J. Tian, *Phys. Rev. B* **76**, 100101(R) (2007).
- [17] X. F. Zhou, Q. R. Qian, J. Zhou, B. Xu, Y. Tian and H. T. Wang, *Phys. Rev. B* **79**,

212102 (2009).

- [18] J. Wang, A. J. Kulkarni, K. Sarasamak, S. Limpijumnong, F. J. Ke, and M. Zhou, Phys. Rev. B **76**, 172103 (2007).
- [19] www.materialsdesign.com; G. Kresse and J. Furthmuller, Software VASP, Vienna, 1999; Phys. Rev. B **54**, 11169 (1996); Comput. Mater. Sci. **6**, 15 (1996).
- [20] S. Fahy, S. G. Louie, and M. L. Cohen, Phys. Rev. B **34**, 1191 (1986); Phys. Rev. B **35**, 7623 (1987).
- [21] Y. Liang, W. Zhang, and L. Chen, Europhys. Lett. **87**, 56003 (2009).
- [22] A. R. Oganov, and C. W. Glass, J. Chem. Phys. **124**, 244704 (2006).
- [23] R. Hill, Proc. Phys. Soc. London **65**, 350 (1952).
- [24] V. V. Brazhkin, A. G. Lyapin, and R. J. Hemley, Philos. Mag. A **82**, 231 (2002).
- [25] F. Gao, J. He, E. Wu, S. Liu, D. Yu, D. Li, S. Zhang, and Y. Tian, Phys. Rev. Lett. **91**, 015502 (2003).
- [26] C. Lee, X. Wei, J. W. Kysar, and J. Hone, Science **321**, 385 (2008).
- [27] X. Blase, P. Gillet, A. S. Miguel, and P. Melinon, Phys. Rev. Lett. **92**, 215505 (2004).

Figure Captions

Fig. 1 (a), (b), and (c) Projection along [100], [010], and [001] directions of $2 \times 2 \times 2$ supercell of Bct-Carbon, the dotted lines in (c) indicate the perpendicular graphene-like structure of Bct-Carbon. (d) Phonon dispersion curve of Bct-Carbon at equilibrium state.

Fig. 2 Calculated total energy versus volume for the Bct-Carbon, M-Carbon, diamond, and graphite; the width of black, red, and blue shadows represent the activation barrier of Bct-Carbon, M-Carbon, and diamond, respectively. The inset shows the enthalpies per atom of Bct-Carbon, and M-Carbon as a function of pressure with respect to graphite.

Fig. 3 (a), (b) The simulated XRD patterns ($\lambda = 0.3329 \text{ \AA}$) of Bct-Carbon, M-Carbon, and graphite at 23.9 and 18.4 GPa with the constant weight. (c) The simulated XRD patterns of pure graphite at 3.3, 13.7 GPa. (d) Experimental data from Ref. 4.

Fig. 4 The calculated stress-strain relations of the Bct-Carbon compared with that of diamond, the arrows indicate the ideal strength (including tensile and shear strength). The inset shows the projection of valence charge density difference of Bct-Carbon in (010) plane at largest shear strain; and the white dotted lines imply that new graphene layer will be reformed in this range with increasing the shear stress or strain.

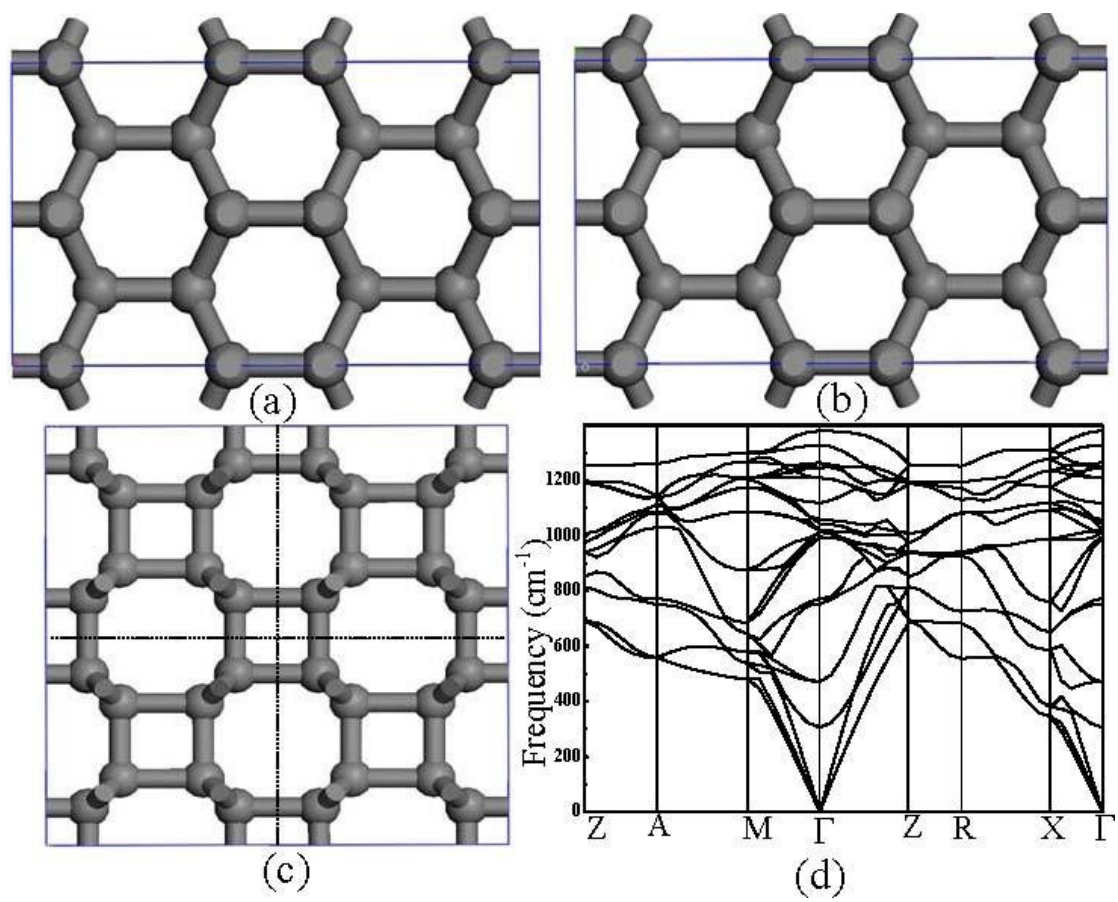


Fig. 1

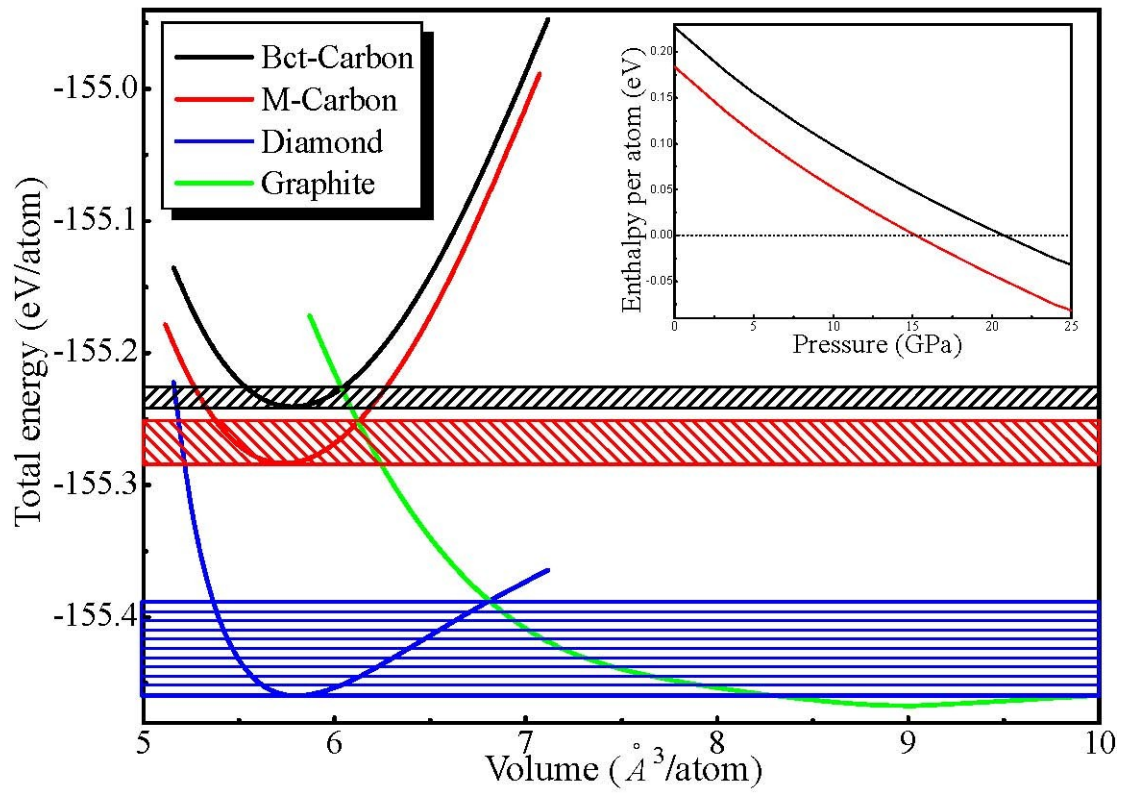


Fig. 2

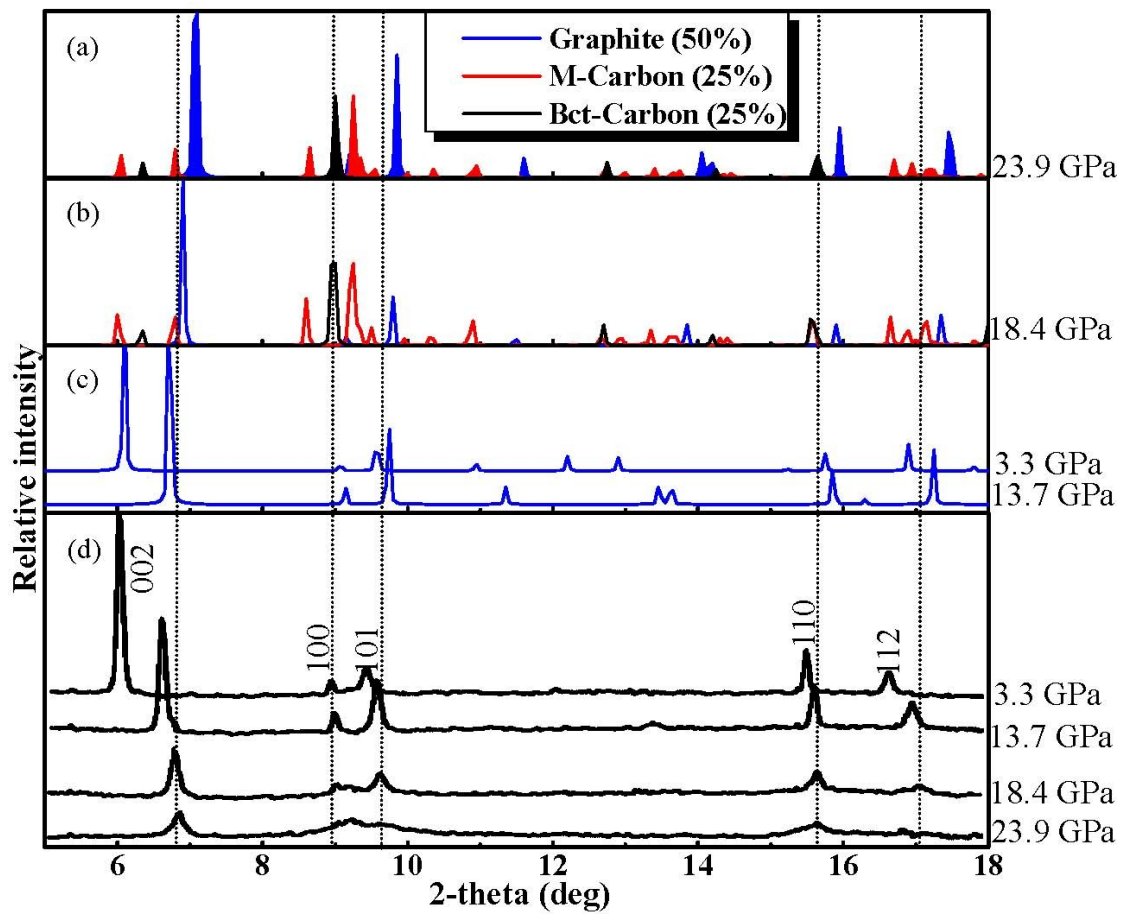


Fig. 3

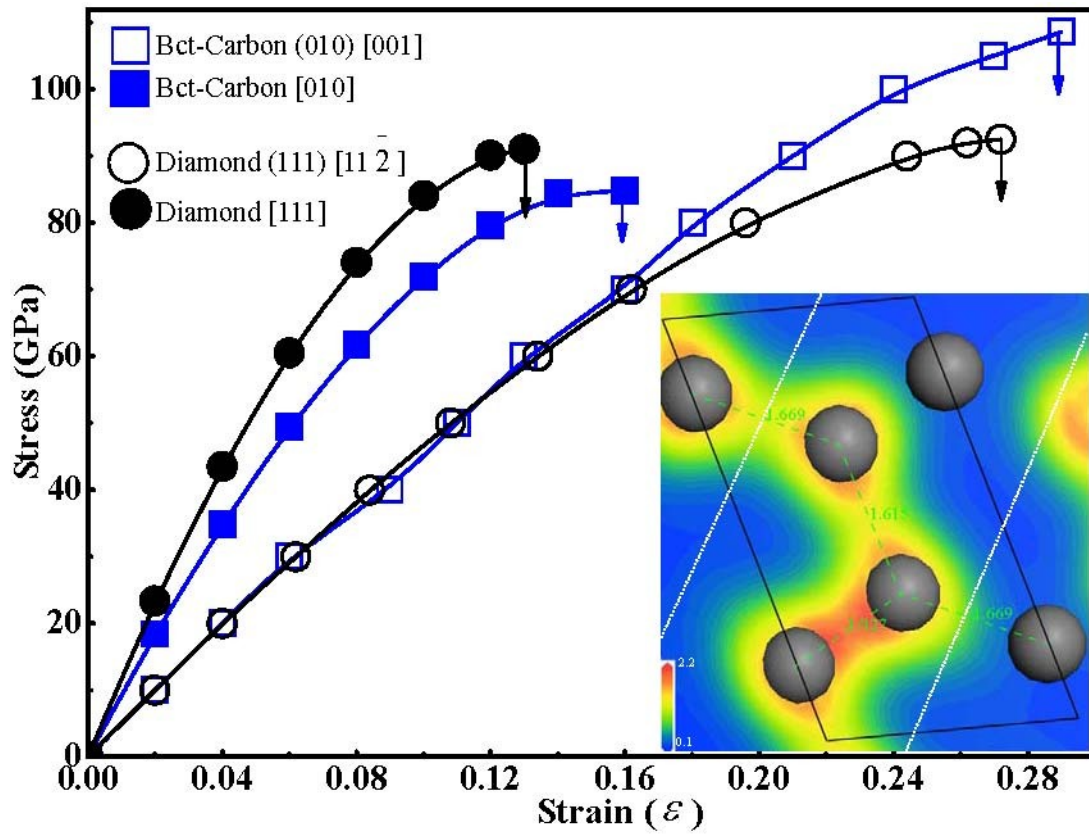


Fig. 4